ERS Scatterometer Observations of Airflow Around Mountainous Islands

Andrew K. Laing — National Institute of Water and Atmospheric Research (NIWA)

Michael J. Revell — P.O. Box 14-901 Kilbirnie, Wellington, New Zealand

a.laing@niwa.cri.nz

Erick Brenstrum — Meteorological Service of New Zealand,

P.O. Box 722, Wellington, New Zealand

Abstract

In regions where mountainous islands strongly influence the airflow, winds from the ERS scatterometers are better able to resolve features in the marine winds than either general ship reports or operational synoptic-scale models. The scatterometer data are used near New Zealand to detail localised intensification in winds due to the orography. The detail is sufficient to show that this effect and its intensity are dependent on the stability of the airflow. A meso-scale numerical model of the New Zealand region is also used to simulate the airflow and results compare very favourably with the scatterometer observations. In low Froude number flows (≈ 0.4) there is substantial blocking and intense jets of wind formed at the ends of the mountain ranges. In higher Froude number flows (≈ 1.0) there is not much evidence for such features.

Keywords: Scatterometer, wind jets, blocking, meso-scale model

Introduction

Satellite-based wind scatterometer data provide an opportunity to observe in detail wind patterns over the oceans. The ERS-1 data have already revealed interesting detail of wind patterns over New Zealand waters (Laing 1994, Laing and Brenstrum 1996), including intense wind enhancement around the ends of large orographic features.

Strong winds in coastal waters may result from a number of processes that affect winds near mountainous islands. The present observations primarily relate to effects around the ends of high barriers. The interaction of the barrier with the flow generates a lee trough and a tight horizontal pressure gradient around the end of the barrier. In stable air with low inertia the air is blocked. It cannot rise over the barrier so it is forced around the end. The resulting isotriptic (down the pressure gradient) winds may penetrate a considerable distance beyond the barrier, e.g. observations from aircraft of the wake of Hawaii (Smith and Grubisic, 1993) revealed jets where the trade winds stream around the edges of the island, extending up to 200 km beyond the barrier. New Zealand presents a major barrier, with steep mountain ranges extending more than 1200 km across the prevailing westerly air flow. These mountains exceed 3000 m for about 200 km and 2000 m for much of their length.

Observing the flow around mountainous islands has the advantage that the downstream region is free of obstructions. However, over waters around New Zealand, surface-based observations of marine winds have been confined to coastal stations and ships' reports. Hourly reports from the NIWA research vessel *Tangaroa* have provided some useful observations of surface wind jets in coastal waters around New Zealand (Brenstrum,1994). However, in general, neither coastal nor ship observations are adequate for making the appropriate detailed observations. Laing and Brenstrum (1996) have shown that the ERS-1 scatterometer data depict regions of local wind intensification, which support the evidence from the *Tangaroa* data. These features are not observed in the surface fields that are generated by the numerical models used to forecast winds over the New Zealand region. In these operational models New Zealand's orography is represented as a broad ridge less than 600 m in elevation. Hence, the local wind variations near New Zealand's terrain are poorly defined. However, more realistic wind fields over New Zealand waters are now becoming available from mesoscale atmospheric models (e.g. Ridley 1991, Revell et al. 1995).

In the present study we show that the scatterometer data has sufficient detail to enable us to quantify the influence of mountainous islands on the airflow, and a meso-scale model is used to successfully simulate events observed in the scatterometer data.

Data Assessment

Scatterometer data

The main source of data for this study was the fast delivery products from the C-band scatterometer on board the European Remote-sensing Satellites (ERS-1 and ERS-2). Residual errors in the directions were removed by comparing the wind directions with 10-m winds from ECMWF analyses.

Ship data

Ships of opportunity are often the only source of surface-based wind data. Unfortunately, the quality of the observations is variable. More regular, higher quality observations are available from the NIWA research vessel *Tangaroa*. These data are concentrated in New Zealand coastal waters and enable some resolution of wind fields there.

Comparisons between ship and scatterometer data

Comparisons were made between the scatterometer winds and observations from (i) the *Tangaroa* and (ii) all other ships, for the period September 1992 to October 1993 within the area bounded by 50°S, 30°S, 150°E and 175°W. Ten-metre winds from ECMWF analyses were separately interpolated in time and space onto the ships' positions.

a. Tangaroa **b. Other ships**	**ρ**	**rmse** **(ms^{-1})**	**bias** **(ms^{-1})**	**No.**
Scatterometer vs ECMWF				
a.	0.76	2.33	-0.26	364
b.	0.72	2.32	-0.42	2282
b. ≥ 180km	0.76	2.22	-0.68	1664
b. < 180km	0.67	2.47	+0.22	562
Ships vs ECMWF				
a.	0.73	3.69	2.02	694
b.	0.55	3.89	0.91	5108
b. ≥ 180km	0.63	3.20	0.17	3340
b. < 180km	0.55	4.94	2.44	1612
Ships vs Scatterometer				
a.	0.86	3.22	2.19	331
b.	0.70	3.30	1.14	2255
b. ≥ 180km	0.68	3.17	0.95	1703
b. < 180km	0.76	3.67	1.74	552

Table 1: Comparisons of ship, scatterometer and ECMWF winds (Tangaroa: "a", all other ships: "b"). The columns show the correlation coefficient (r), root-mean-square difference (rmse), bias (observations from first source minus the second) and the number of points of comparison.

Some of the statistics of the inter-comparisons are shown in Table 1 (see also Laing and Brenstrum, 1996). These are presented in two bands - beyond 180 km and within 180 km of the New Zealand coast. We see that the wind speeds from ships (especially the Tangaroa) correlate significantly better with scatterometer values than they do with ECMWF. This is consistent with the ECMWF fields being smooth, with errors around meso-scale features, which are captured by both scatterometer and ship observations. The considerably larger gap in the correlations near the coast (0.55 for ships vs ECMWF compared to 0.76 for ships vs scatterometer) compared to those away from the coast (0.63 compared to 0.68) suggests that the scatterometer is relatively more useful for winds close to the coast than ECMWF. It is also evident that ships' observations are higher than ECMWF which are higher than the scatterometer winds by over 0.4 ms^{-1} (0.7 ms^{-1} for >180 km offshore). This is consistent with (i) Quilfen (1992), where they are biased low (compared to buoy measurements) by 0.85 ms^{-1}, and (ii) Stoffelen and Anderson (1994), where the low bias (compared to ECMWF winds) is nearly 0.5 ms^{-1} at the near side of the swath to 0.24 ms^{-1} at the far side. Near land (within 180 km), however, the bias is reversed and the ECMWF winds are slightly lower than scatterometer winds, reflecting over-smooth model wind fields near the coast.

It is a reasonable conclusion (see also Stoffelen and Anderson, 1994) that scatterometer data are more accurate than any other operationally available wind data set, and are particularly suited to observing marine winds near mountainous islands.

Observations of "Rivers of Wind"

ERS-1 scatterometer data depict events in which there is apparent intensification of wind in the lee of orographic features on the New Zealand coast. In Laing and Brenstrum (1996) a total of 78 events were identified at 6 locations during 1993. In the present discussion we will focus on the 25 events associated with the ends of the major mountain chain, viz: Puysegur Point, at the south-west of the South Island, and East Cape at the north-east of the North Island (see Figure 1). Table 2 summarises the relevant wind features.

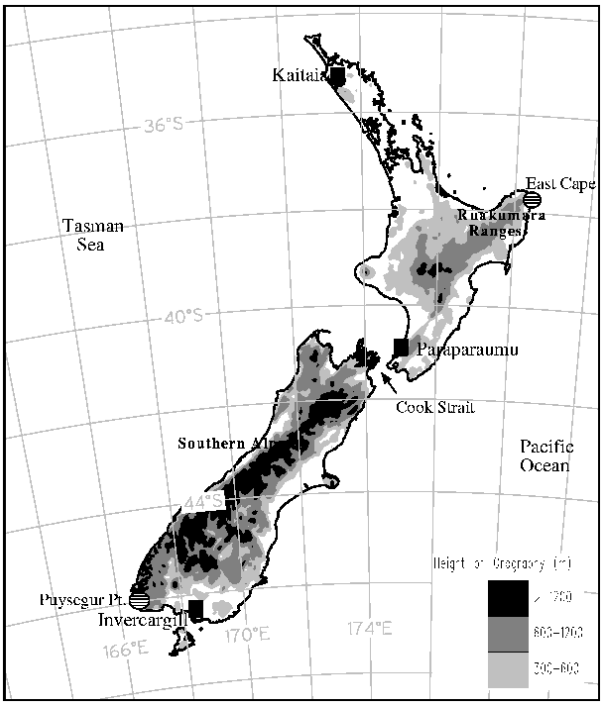

Figure 1: Map of New Zealand showing the three radiosonde stations (■), the locations for the "Rivers of wind" events (◍) and major orographic features.

	Puysegur Pt	**East Cape**
Number	16	20
Length (km)	300	230
Width (km)	120	200
Orientation	355°	90°
Dist. from land (km)	80	200
N (0.01 s^{-1})	1.26	1.19
N range (0.01 s^{-1})	1.00-1.57	0.92-1.57
Fr	0.25	0.43
Burger	5.0	6.3

Table 2: Summary of low -level wind jets at East Cape and Puysegur Point. The rows show the mean length, width and orientation of the features, mean distance from the coast, mean Brunt-Väisälä frequency (0.01s^{-1}), range of frequencies, mean Froude Number and mean Burger number.

Characterisation

The midpoint between the maximum wind speed and the ambient synoptic wind was used to delineate the feature and give a characteristic wind speed. The associated isotach allows width and length scales to be measured. The intensity, or enhancement (*E*), was then calculated as the percentage increase in the characteristic speed of the feature above the ambient wind speed.

Stability characteristics for these events are determined from radiosonde data from the nearest meteorological observatory (see Figure 1). The mean Brunt-Väisälä frequency (*N*) for dry air was calculated over a depth of atmosphere (*H*) commensurate with the height of the main orographic feature. The Froude number *Fr = U/ HN*, where *U* is the geostrophic wind speed near the barrier, inversely measures the blocking tendency.

Puysegur Point

At the southwest corner of New Zealand the mountain chain ends abruptly at the coast. The mountains rise to nearly 2000m directly inland from Puysegur Point, and to over 2500m further north, providing a continuous, long barrier (see Figure 1). Stability characteristics were determined from Invercargill radiosonde data (se Figure 1) and a scale height of 2500m, appropriate for the central Southern Alps, was used in calculating the mean Brunt-Väisälä frequency (*N*). The general synoptic situation favoured for events here is anticyclonic, with a south to southeasterly flow over the South Island of New Zealand. A lee trough then extends along the western coast of the South Island.

The 15 wind features examined were all centred quite close to land, and penetrated a large distance into the eastern Tasman Sea. Unfortunately, in many cases the feature was not completely within the scatterometer swath so the mean length will be actually be greater than the value quoted in Table 2.

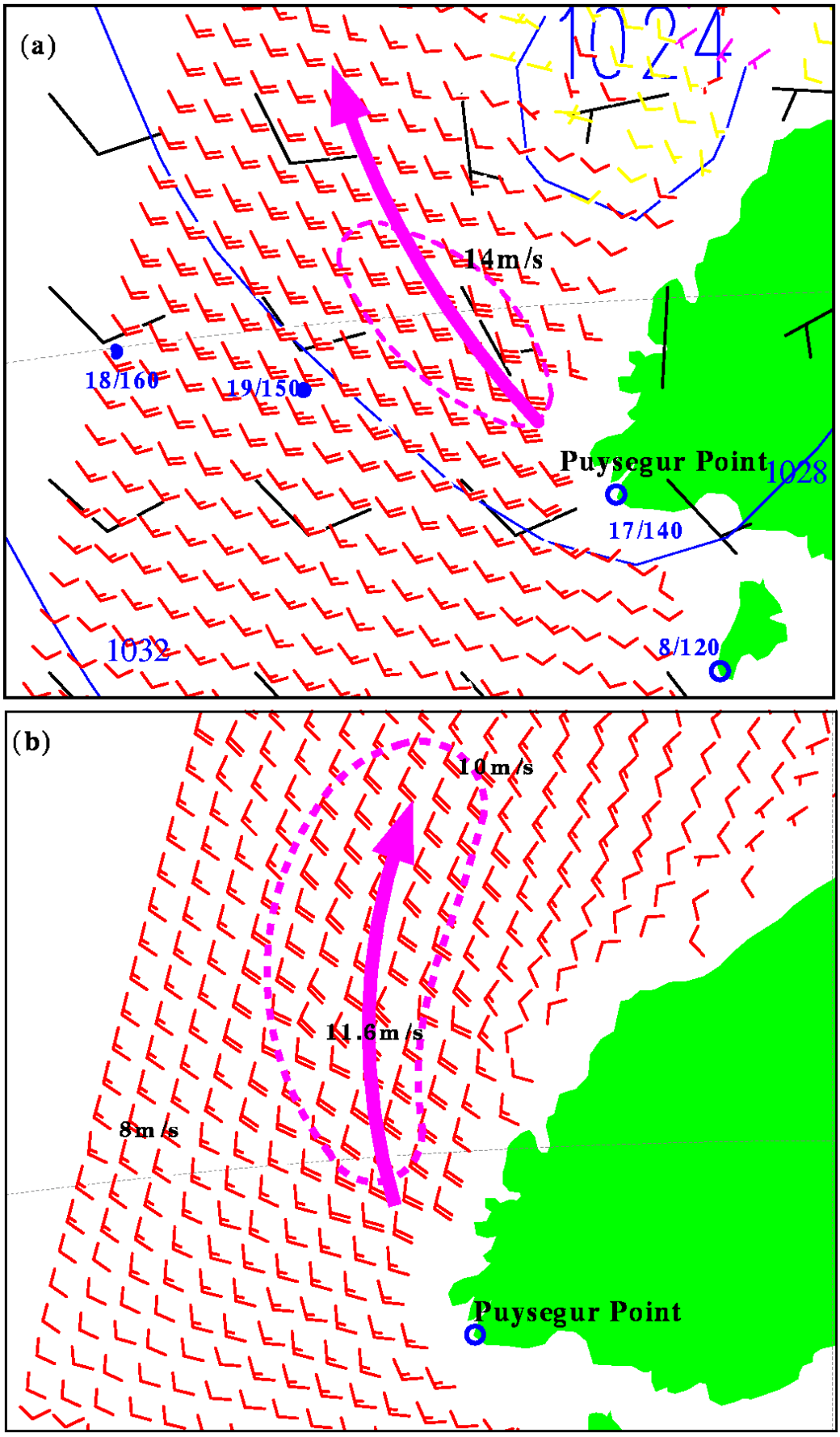

Figure 2: Scatterometer winds for (a) the ERS-1 pass at 2230UTC on September 5, 1993. Full barbs indicate 10 knots (5 ms^{-1}), half-barbs indicate 5 knots (2.5 ms^{-1}). Also shown are the 14 ms^{-1} (27 knot) isotach (thick dashed line), the line of the wind maximum (thick arrowed line), the wind observations at Puysegur Point and two concurrent ship observations (formatted as knots/direction). Isobars (values in hPa) from the ECMWF surface pressure field for 0000UTC on September 6 are drawn as solid black lines. (b) the ERS-2 pass at 2225UTC on November 8, 1996, with 10ms^{-1} isotach.

A typical situation off Puysegur Point occurred on September 6, 1993. The scatterometer data (see Figure 2a) show a large area of enhanced winds. These stronger winds were surrounded by ambient winds of 5 ms^{-1} to 8 ms^{-1} (10 knots to 15 knots). Reports from two ships within the area were consistent with the scatterometer data. The radiosonde data for 0000UTC indicated high stability with a mean N of 0.0146 s^{-1} (considerably above the mean of 0.011 s^{-1}). The low Fr of 0.22 reflects strong blocking.

In Figure 2b a similar case with a more southerly ambient flow is depicted, for November 9, 1996. The ERS-2 scatterometer data clearly depict an extensive feature. In this case the enhancement is modest, at about 0.7 (1.7 times the ambient flow) with a peak at about double the ambient speed.

East Cape

In west-south-westerly flows the Ruakumara ranges, at the north-eastern end of the main mountain chain, cause a lee trough to form to the east of East Cape (see Figure 1). An enhanced flow then streams eastwards offshore from the northeastern corner of the North Island. A total of 20 such events were selected for 1993, all centred about 100 km from East Cape.

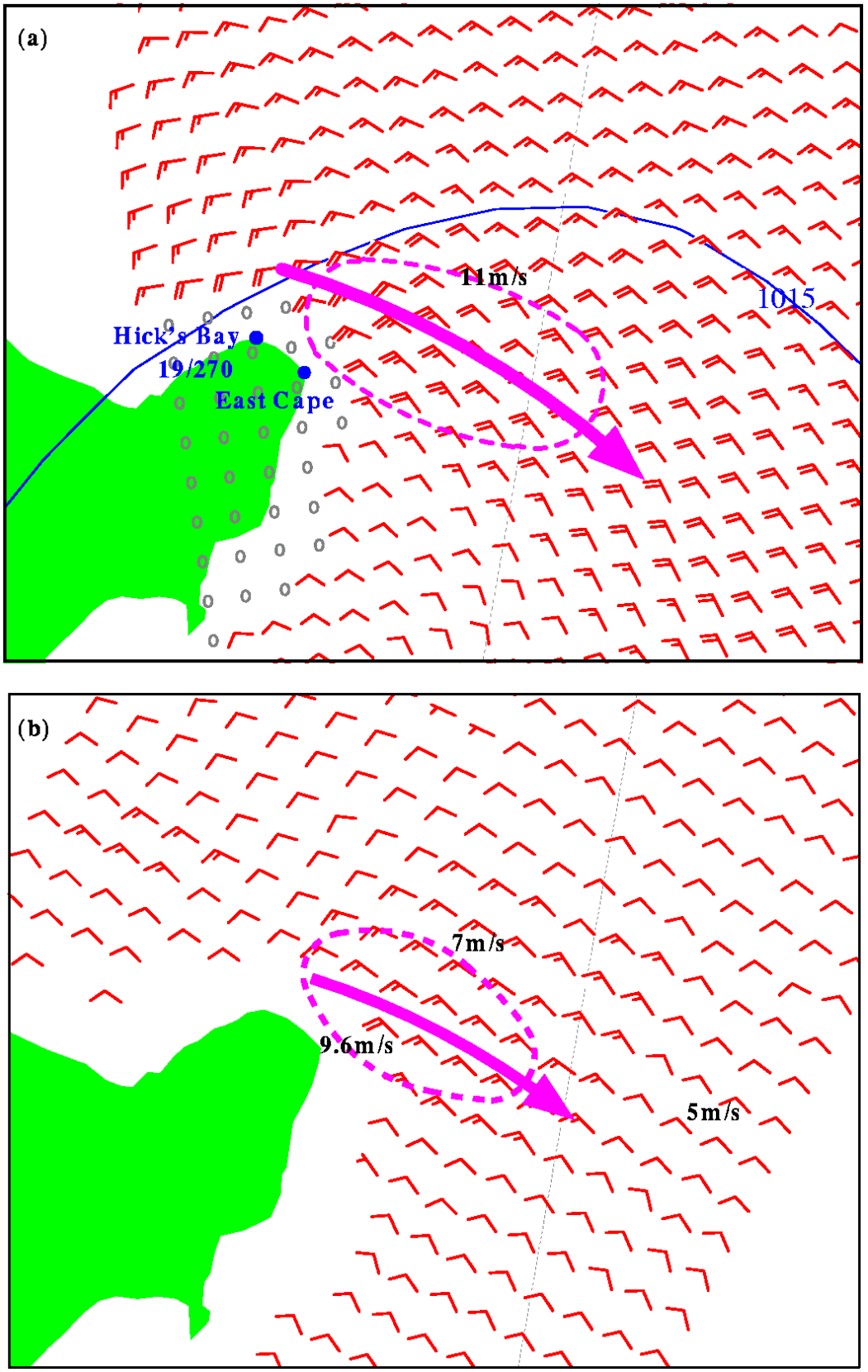

Figure 3: Scatterometer winds (as in Figure 2) for (a) the ERS-1 pass at 1115UTC on October 13, 1993. Also shown are the 11 ms^{-1} (21 knot) isotach (the grey dashed line), the line of the wind maximum (the thick grey line) and the wind observation for Hick's Bay. The ECMWF isobars are for 1200UTC. (b) for ERS-2 pass at 2145UTC on October 2, 1996, with 7 ms^{-1} isotach.

The feature off East Cape on October 13th, 1993, was typical for this location. At 1200UTC on October 13, 1993 the radiosonde data from Paraparaumu showed a stable atmosphere at all heights with a marked stable layer between 1700 m and 2600 m (the scale height used for the ranges here is 1500 m). The mean N in the lower 2000 m was 0.011 s^{-1} and $Fr \approx 0.4$. The scatterometer data in Figure 3 show an elongated area of 13 ms^{-1} (25 knot) winds about 200 km long and 50 km wide extending eastwards from East Cape. Ambient winds surrounding this area were 8 ms^{-1} (15 knots).

This case is similar to one reported by Brenstrum (1994) when the ship *Tangaroa* was in the area and reported westerly winds of 15 to 21 ms^{-1} (30 to 40 knots) over a number of hours (Figure 4).

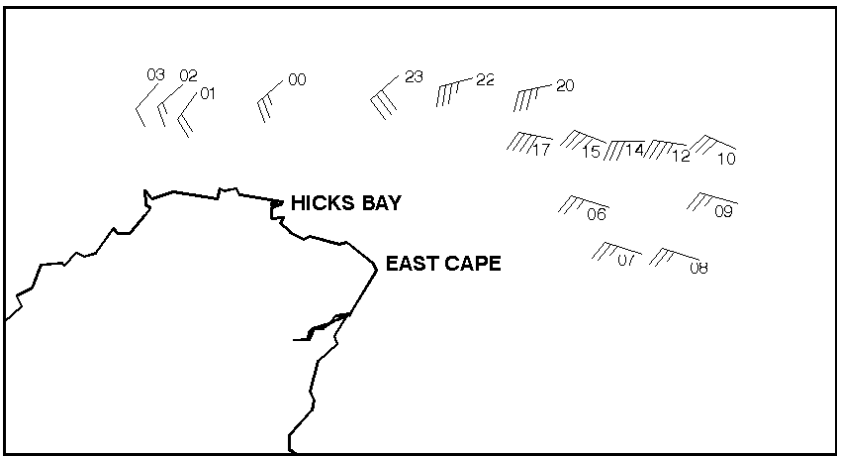

Figure 4: Tangaroa observations of winds off East Cape. The time of each observation is indicated as hours UTC on March 24 - 25, 1992 (moving from right to left). The wind barbs are as in Figure 2.

In Figure 3b a similar case in a westerly flow on October 3, 1996, from the ERS-2 scatterometer is shown. The maximum wind-speed of 9.6ms^{-1} is quite close to the coast.

Blocking

In the present cases the air was invariably very stable. For the sample of 78 events investigated by Laing and Brenstrum (1996), the *Fr* are all < 1.0 and only 4 events occurred with *Fr*>0.7. Most (74%) were lower than 0.5. Indeed, they showed that the sample of events are drawn from a stable sub-population with low *Fr*. In this sub-population there is a distinct transition from a higher than normal occurrence of the *Fr* value at *Fr*<0.7 to lower occurrence than normal for *Fr*>0.7.

For the present sample the intensity, measured by the fractional increase in the wind speed of the jet over the surrounding winds, is plotted against *Fr* in Figure 5, showing an inverse relationship. The correlation between intensity and 1/*Fr* is 0.77, (59% explained variance). Smith and Grubisic (1993) measured a doubling of the trade wind speed around Hawaii in conditions of an average *Fr* ~ 0.5 (for saturated air). This is comparable to the present study where an enhancement of 1.0 (see Figure 5) is measured for *Fr* ~ 0.2-0.4.

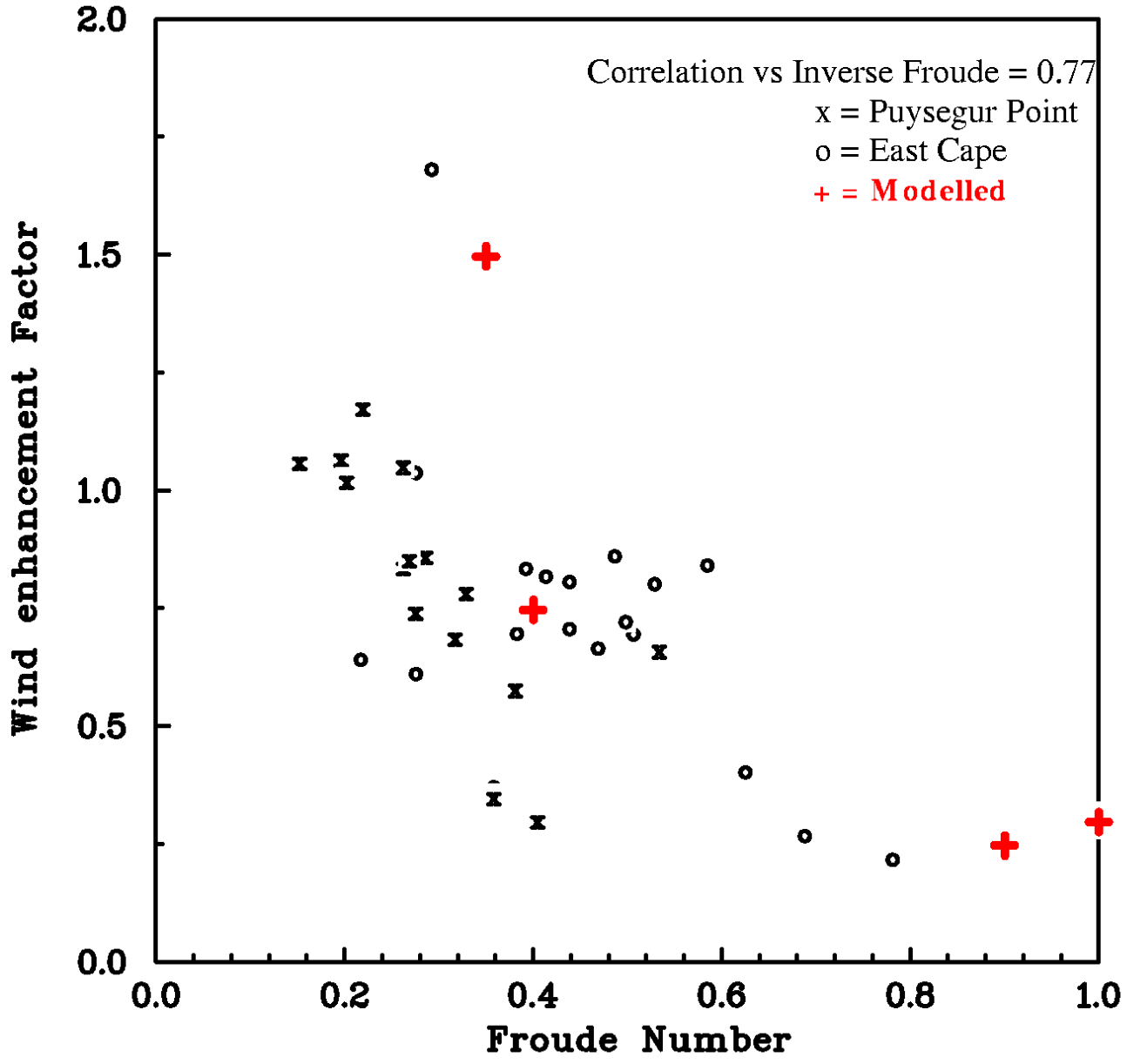

Figure 5: Scatter plot of enhancement factor (fractional speed-up of the wind in a "river of wind" over the surrounding wind speeds) versus Froude number for events near Puysegur Point ("x") and near East Cape ("o"). The results from the model runs are indicated with "+".

Model Simulations

Having derived some criteria for formation of these jets, we attempt to simulate them using a meso-scale numerical model. Our hypothesis was that the presence and intensity of these "rivers of wind" could be explained predominantly by varying *Fr*. High values of *Fr* correspond to strong winds, low stability and low hills, when we expect the deviation of the flow by the orography to be small. Contrastingly, for low values of *Fr*, corresponding to lighter winds more stable conditions and higher mountains, we expect much larger deviation of the flow by the orography.

We used version 3b of the RAMS model described in Pielke et al. (1992). The model had three levels of nesting with corresponding grid sizes of 80, 20 and 5 km. The 80km grid covered the entire region extending to Australia in the west, the 20 km grid included the area in Figure 1 and the 5 km grid corresponded the areas shown in Figures 6 and 7 for the north-east and south-west of the country respectively. In order to isolate this Froude number effect we kept our initial conditions simple. The model had initial relative humidity set to 40% everywhere and did not employ moist physics. Using starting fields that were initially horizontally homogeneous, with constant wind speed and direction as a function of height, a constant N below 250 hPa and isothermal conditions above, we ran the model for four regimes. The first two are for small and large Fr at East Cape and the last two similarly at Puysegur point:

1a. West-southwesterly with Fr = 0.4, U=[250° ,9.0 ms^{-1}], N=0.014 s^{-1}, H=1600 m

1b. West-southwesterly with Fr = 0.9, U=[250° ,10.1 ms^{-1}], N=0.007 s^{-1}, H=1600 m

2a. Southeasterly with Fr = 0.32, U=[130° ,9.0 ms^{-1}], N=0.014 s^{-1}, H=2000 m

2b. Southeasterly with Fr = 1.07, U=[130° ,11.25 ms^{-1}], N=0.007 s^{-1}, H=2000 m

The model was run for 12 hours in each case, as this seemed to be the time needed for the model to establish a new equilibrium. A typical scenario was for strong winds to be generated just off the headlands in the first hour of integration, and as advective and Coriolis forces took effect a jet was established downstream and further off the coast. A turning of the wind clockwise by some 20° due to friction in the lowest layer also occurred during this time.

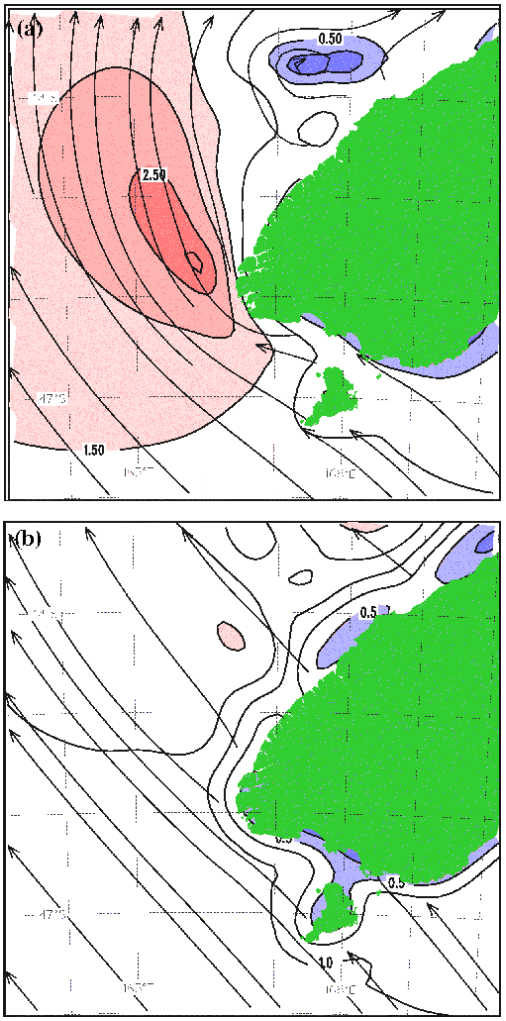

Figure 6: RAMS simulation of south-easterly flow past Puysegur Point. Contours are fractional speed up (in 0.5 intervals, plus 0.25 and 2.75). Flow direction is indicated by the streamlines (with arrows). (a) Blocked stable flow with Fr = 0.35, (b) Unblocked flow with Fr = 1.0.

Our results shown in Figure 6 for Puysegur Point and Figure 7 for East Cape are in very good agreement with the scatterometer observations in Figure 2 and Figure 3 respectively.

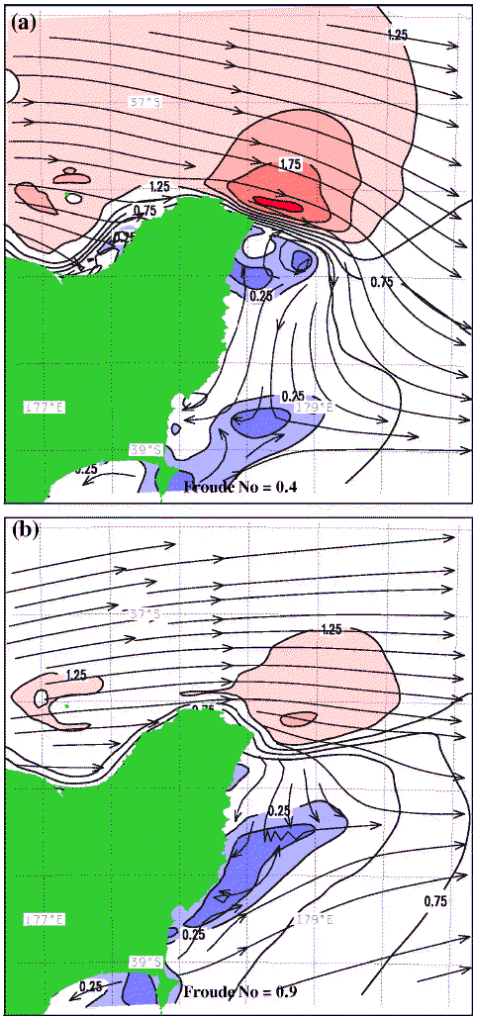

Figure 7: RAMS simulation of westerly flow past East Cape. Contours are fractional speed up (in 0.25 intervals). Flow direction is indicated by the streamlines (with arrows). (a) Blocked stable flow with Fr =0.4, (b) Unblocked flow with Fr = 0.9.

Both the location and fractional speed-up as a function of the *Fr* of the "rivers of wind" predicted by the model correspond closely to the satellite data. The 4 modelled cases have been included in the plot of the fractional speed up as a function of inverse Froude number in Figure 5. These values fit very well within the observed data.

Conclusions

The ERS scatterometer data resolve wind fields in coastal waters around New Zealand better than operational numerical analyses or ships' observations. Whilst the scatterometer swaths only provide intermittent coverage, they add a spatial dimension which is precluded from ships' observations by their low density and from operational model analyses by their inadequate resolution.

The Tangaroa data have occasionally exposed low-level wind jets streaming around the edges of prominent orographic features. The scatterometer data confirm these features and depict further characteristics. They appear in stable, well-blocked airflow with Fr< 0.7. Stronger blocking generates more intense low-level jets. These deductions are further tested and confirmed by simulations using a high-resolution meso-scale model.

Acknowledgments

This research was carried out under Foundation for Research, Science and Technology contract CO1521. We would also like to thank the European Space Agency (ESA) for access to the ERS-1 and ERS-2 data.

References

Brenstrum, E.M., 1994:

Coastal wind patterns revealed by hourly reports from a ship at sea, *Weather and Climate*, **14**(1), 16-23.

Laing, A.K., 1994: Features of marine wind fields over New Zealand waters from ERS-1 scatterometer data. *N.Z. J. of Marine and Freshwater Res*., **28**, 365-378

Laing, A.K., and E. Brenstrum, 1996: Scatterometer observations of low-level winds jets over New Zealand coastal waters. *Weather and Forecasting*, **11**(4), 458-475.

Pielke, R.A., W.R. Cotton, R.L. Walko, C.J. Tremback, W.A. Lyons, L.D. Grasso, M.E. Nicholls, M.D. Moran, D.A. Wesley, T.J. Lee, and J.H. Copeland, 1992: A comprehensive meteorological modelling system - RAMS. *Meteor. Atmos. Phys*., **49**, 69-91.

Quilfen, Y. 1992: Validation and quality of ERS-1 data: Scatterometer wind data. *Proc. of the ERS-1 geophysical validation workshop*, Penhors France, 27-30 April, 1992, 107-112.

Revell, M.J., M.R. Sinclair and D.S. Wratt, 1995: The storm of November 1994: Numerical simulation of a heavy rain event over the Southern Alps of New Zealand, using the RAMS model at very high resolution. *Proc. GEWEX Workshop on clouds*, New York.

Ridley, R.N. 1991: Observation and numerical modelling of airflows over New Zealand. Ph.D. Thesis, Monash University, Melbourne, Australia.

Smith, R.B., 1979: The influence of mountains on the atmosphere. *Advances in Geophysics*, **12**, 87-230..

Smith, R.B. and V. Grubisic, 1993: Aerial observations of Hawaii's wake. *J. Atmos. Sci*., **50**, 3728-3750.

Stoffelen, A. and D.L.T. Anderson, 1994: Characterisation of ERS-1 scatterometer measurements and wind retrieval. *Proc. of the Second ERS-1 symposium - Space at the service of our environment*, Hamburg, Germany, 11-14 Oct. 1993, pp 997-1001.n, 1995a